Yeast Orotidine-5′-Phosphate Decarboxylase: Steady-State and Pre-Steady-State Analysis of the Kinetic Mechanism of Substrate Decarboxylation

David J. T. Porter* and Steven A. Short

Glaxo Wellcome, 5 Moore Drive, Research Triangle Park, North Carolina 27709

Received May 25, 2000

ABSTRACT: The catalytically active form of monofunctional yeast orotidine-5′-phosphate decarboxylase was a dimer (E_2). The dimer equilibrium dissociation constant was 0.25 μM in 0.01 M MOPS Na^+ at pH 7.2. The bimolecular rate constant for dimer formation was 1.56 μM^{-1} s^{-1}. The dimeric form of the enzyme was stabilized by NaCl such that the enzyme was E_2 in 100 mM NaCl at all concentrations of enzyme tested. The kinetics of binding of OMP to E_2 was governed by two ionizations ($pK_1 = 6.1$ and $pK_2 = 7.7$). From studies with substrate analogues, the higher p*K* was assigned to a group on the enzyme that interacted with the pyrimidinyl moiety. The value of the lower p*K* was dependent on the substrate analogue, which suggested that it was not exclusively the result of ionization of the phosphoryl moiety. During the decarboxylation of OMP, the fluorescence of E_2 was quenched over 20%. The enzymatic species with reduced fluorescence was a catalytically competent intermediate that had kinetic properties consistent with it being the initial enzyme−substrate complex. The stoichiometry for binding of OMP to E_2 was one OMP per enzyme monomer. The value of the first-order rate constant for conversion of the enzyme−substrate complex to free enzyme (36 s^{-1}) calculated from a single turnover experiment ([E] ≫ [S]) was slightly greater than the value of k_{cat}, 20 s^{-1} (corrected for stoichiometry), calculated from steady-state data. In the single turnover experiments, the enzyme was E_2•S, whereas in the steady-state turnover the experiment enzyme was E_2•S_2. The similarity of these values suggested that the subunits were catalytically independent such that E_2•S_2 could be treated as E•S and that conversion of the enzyme−substrate complex to E was k_{cat}. Kinetic data for the approach to the steady-state with OMP and E_2 yield a bimolecular association rate complex of 62 μM^{-1} $s^{-1}$and a dissociation rate constant for E•S of 60 s^{-1}. The commitment to catalysis was 0.25. By monitoring the effect of carbonic anhydrase on [H^+] changes during a single turnover experiment, the initial product of the decarboxylation reaction was shown to be CO_2 not HCO_3^-. UMP was released from the enzyme concomitantly with CO_2 during the conversion of E•S to E. Furthermore, the enzyme removed an enzyme equivalent of H^+ from solvent during this step of the reaction. The bimolecular rate constants for association of 6-AzaUMP and 8-AzaXMP, substrate analogues with markedly different nucleobases, had association rate constants of 112 and 130 μM^{-1} s^{-1}, respectively. These results suggested that the nucleobase did not contribute significantly to the success of formation of the initial enzyme−substrate complex.

Orotidine-5′-phosphate decarboxylase (EC 4.1.1.23, ODCase)[1] is an essential enzyme that catalyzes the conversion of OMP to UMP (*1*). The first-order rate constant for decarboxylation of OMP in the E−OMP complex is 1.4×10^{17}-fold faster than in a physiological buffer (*2*). The enzyme isolated from *Saccharomyces cerevisiae* has been demonstrated not to contain a metal cofactor (*3*, *4*). Steady-state kinetic analysis of the enzyme (*5*−*8*) and studies on the state of aggregation have been reported (*9*). However, suggestions as to the mechanism of this extraordinary rate enhancement by ODCase have been based largely on the results from model studies. Beak and Seigel proposed a zwitterion mechanism in which a cationic nitrogen at N-1 stabilizes the incipient carbanionic intermediate generated at C-6 during the decarboxylation reaction (*10*). Lee and Houk have proposed a carbene mechanism in which protonation of O-4 could stabilize a carbene-like intermediate at C-6 (*11*). Finally, Silverman and Groziak have proposed covalent catalysis mechanism involving nucleophilic attack at C-5 by an enzymatic group with protonation of C-6 prior to decar-

* To whom correspondence should be addressed. Telephone: (919) 483−4390. FAX: (919) 483-3895. E-mail: djp39807@glaxowellcome.com.

[1] Abbreviations: 6-azaUMP, 6-azauridine monophosphate; 6-NH_2C-(S)UMP, 6-thiocarboxamidouridine 5′-phosphate; UMP, uridine 5′-phosphate; OMP, orotidine 5′-phosphate; BMP, 1-(5′-phospho-β-D-ribofuranosyl)barbituric acid; dUMP, deoxyuridine 5′-phosphate; FdUMP, 5-fluorodeoxyuridine 5′-phosphate; OxypurinolMP, oxypurinol 5′-phosphate; 8-AzaXMP, 8-azaxanthosine 5′-phosphate; AllopurinolMP, allopurinol 5′-phosphate; ThiopurinolMP, thiopurinol 5′-phosphate; ODCase, orotidine-5′-phosphate decarboxylase without regard to the state of aggregation of the enzyme; E, monomeric orotidine-5′-phosphate decarboxylase; E_2, dimeric orotidine-5′-phosphate decarboxylase; E_2S, dimeric orotidine-5′-phosphate decarboxylase with one site occupied by S; E_2S_2, dimeric orotidine-5′-phosphate decarboxylase with both sites occupied by S; k_1, bimolecular association rate constant for enzyme and ligand; k_{-1}, dissociation rate constant of the enzyme-ligand complex; K_d, equilibrium dissociation constant for enzyme and ligand; K_i, kinetic inhibition constant; pK_1, proton ionization constant of ligand or enzyme; pK_2, proton ionization constant of ligand or enzyme; MOPS, 3-(*N*-morpholino)propanesulfonic acid; CHES, 2-(*N*-cyclohexylamino)ethanesulfonic acid; TRICINE, *N*-tris(hydroxymethyl)glycine; CAPS, 3-(cyclohexylamino)-1-propanesulfonic acid; BCECF, 2′,7′-bis-(2-carboxyethyl)-5 (and -6)-carboxyfluorescein.

10.1021/bi001199v CCC: $19.00
Published on Web 08/25/2000

boxylation (*12*). Data on kinetic isotope effects (*13*−*15*) and substrate analogues (*16*, *17*) did not support a covalent catalysis mechanism.

ODCase activity from microbial sources resides in a monofunctional protein in contrast to the multifunctional protein from mammalian sources (*18*). Recently, X-ray crystallographic structures of ODCase from three microbial sources have been reported. The structures of the enzyme from *S. cerevisiae* have been solved in the presence and absence of a substrate analogue (*19*). Using protein from *Bacillus subtilis*, Appleby et al. (*20*) proposed an S_E2 mechanism in which a lysyl residue of the enzyme near C-6 donates a hydrogen ion concertedly with decarboxylation. A combination of solvent and substrate ^{13}C kinetic isotope effects on *V*/*K* for *Escherichia coli* ODCase suggested that decarboxylation and proton transfer occur in separate steps (*15*). These results were not consistent with the S_E2 mechanism proposed by Appleby et al. (*20*) but were interpreted as supporting the carbene mechanism of Lee and Houk (*11*). However, Appleby et al. (*20*) have suggested that the solvent isotope effect results were not diagnostic and could be explained if a substantial fraction were the result of substrate binding or a protein conformational change. On the basis of the crystal structure of the enzyme from *S. cerevisiae* complexed with BMP, Miller et al. (*19*) proposed the zwitterionic mechanism of Beak and Siegel (*10*). Finally, from the crystal structure of the enzyme from *Methanobacterium thermoautotrophicium* complexed with 6-AzaUMP, Wu et al. (*21*) have proposed that destabilization of ground state plays a predominate role in the catalytic mechanism. Model studies have been reported supporting the destabilization of the ground-state model (*22*).

Despite the elegant studies reported above on the mechanism of decarboxylation of OMP by ODCase from microbial sources, a consensus kinetic and chemical mechanism is lacking. However, the data presently available favor an electrostatic mechanism over a covalent mechanism. Because of the many mechanistic questions remaining unanswered, we initiated a detailed study of the steady-state and pre-steady-state kinetics for the interaction of the *S. cerevisiae* enzyme with OMP and substrate analogues to address the following points of the kinetic mechanism of this enzyme: (i) the relative catalytic activities of the monomeric and dimeric forms of the enzyme, (ii) the interaction between the subunits in the dimeric enzyme, (iii) whether CO_2 or HCO_3^- is released from the enzyme, (iv) at what stages of the catalytic cycle H^+ is removed from solvent and when CO_2 and UMP are released from the enzyme, and (v) interpretation of the pH rate profile for the bimolecular association rate constants for substrate and substrate analogues.

EXPERIMENTAL PROCEDURES

Materials. MOPS, OMP, UMP, 6-AzaUMP R-5-P, XMP, dUMP, FdUMP, MOPS, MES, CHES, sodium acetate, TRICINE, CAPS, and carbonic anhydrase were from Sigma-Aldrich (St. Louis, MO). BCECF was from Molecular Probes (Eugene, OR). 8-AzaXMP, AllopurinolMP, ThiopurinolMP, and OxypurinolMP were from the Burroughs Wellcome compound collection.

General Methods. The standard buffer was 0.01 M MOPS (Na^+) with 100 mM NaCl at pH 7.2. The standard temperature was 25 °C. Steady-state fluorescence data were collected with a Kontron SFM 25 spectrofluorometer using λ_{ex} = 280−305 nm and λ_{em} = 340−350 nm. Fluorescence time courses presented were representative of at least three experiments. Rapid reactions were monitored with an Applied Photophysics SX.17MV spectrophotometer SX.17MV (Leatherhead, UK). Absorbance data was collected with a slit width of 2 mm and a path length of 10 mm. Fluorescence data was collected with a slit width of 2 mm, an excitation path length of 2 mm and λ_{ex} = 280 nm and λ_{em} > 320 nm. Conventional kinetic data were obtained from a UVIKON 860 spectrophotometer. Equations described below were fitted to the data by nonlinear least squares using SigmaPlot from Jandel Scientific (Corte Madera, CA). The fits of the parameters to the data are reported as the fitted value with the standard error of the least significant figure in parentheses.

Preparation of Enzyme. The enzyme was prepared as described previously (*3*). The enzyme was stored at −10 °C in 50 mM Tris-HCl, 20% glycerol, 5 mM β-mercaptoethanol at pH 7.5. The enzyme buffer was changed to the standard buffer by size exclusion chromatography through a 5-mL column of Bio-Rad P-6 resin equilibrated in the standard buffer. Enzyme concentrations are expressed in terms of subunit concentration that was calculated from the absorbance of the enzyme solution at 280 nm and ϵ_{280} = 28.8 mM^{-1} cm^{-1}. Quantitative amino acid analysis gave ϵ_{280} = 32.3 (5) mM^{-1} cm^{-1} (N = 3).

Assay of the Enzyme. The concentration of OMP prepared gravimetrically from commercially available OMP was estimated spectrophotometically from the absorbance at 267 nm in 100 mM HCl and the extinction coefficient of orotidine (9.57 mM^{-1} cm^{-1}, Calbiochem). The concentration calculated from spectrophotometric data and that calculated from gravimetric data agreed within 5%. The change in extinction coefficient for the conversion of OMP to UMP was determined from the absorbance change of a solution of OMP after decarboxylation with enzyme. The maximal absorbance change was at 279 nm. The value of $\Delta\epsilon_{279}$ from four independent determinations was 2.4 ± 0.2 mM^{-1} cm^{-1}. The standard assay monitored the decarboxylation of 20 μM OMP in the standard buffer. The reaction was initiated by 100-fold dilution of stock enzyme solution (∼5 μM) prepared in the standard buffer. The turnover number of the enzyme was typically between 14 and 18 s^{-1}.

Determination of Kinetic Parameters for Substrate-Induced Dimerization of E. Selected concentrations of enzyme were equilibrated in the standard buffer or standard buffer in the absence of NaCl for 30−60 s prior to initiation of the reaction with OMP. The decarboxylation of OMP was monitored spectrophotometrically at 279 nm. For long time courses (>40 s), the UVIKON 860 spectrophotometer was used to monitor product, whereas for short time courses in which initial velocities were determined, the stopped-flow spectrophotometer was used to monitor product. In the former experiments, the concentration of enzyme in the decarboxylation reaction was equal to the concentration of enzyme in the preequilibration mixture. In the latter experiment, the concentration of enzyme in the decarboxylation reaction was half of that in the preequilibration mixture because of a 1 to 1 dilution that occurred upon mixing substrate with enzyme. These data were analyzed according to the simplified dimerization model described by Scheme 1.

Scheme 1: Simplified Model for Dimerization of E to the Catalytically Active Form (E_2) in the Presence of Substrate

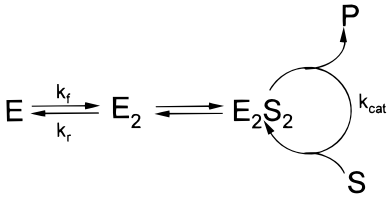

For derivation of equations describing this model, the substrate concentration was much greater than the K_m such that only E and E_2S_2 were present at significant concentration during the experiment so that k_r does not contribute to the kinetic process after addition of substrate. Evidence is presented in Results that only E_2 binds substrate. The expression for the time course for decarboxylation of OMP by a solution of enzyme that was initially monomeric is described by eq 1 where $[E_T]$ is the total subunit concentration. Derivation of this equation involved a double integration. The expression for the time course for formation of E_2S_2 from E was determined by integration of the differential equation describing the disappearance of E ($-k_f[E]^2$) and the conservation of E_T. Integration of the expression for the rate of product formation ($k_{cat}[E_2S_2]$) yielded eq 1.

$$[UMP(t)] = k_{cat}[E_T]t - \frac{k_{cat}}{k_f}\ln(k_f t E_T + 1) \quad (1)$$

The dependence of the initial velocity of OMP decarboxylation on $[E_T]$ is given by eq 2. The derivation of this equation is analogous to that described by Gittelman and Matthews (*23*). In these experiments, $[E_T]$ is the subunit

$$V_0 = \frac{k_{cat}}{8}[(4[E_T] + K) - \sqrt{(4[E_T] + K)^2 - 16[E_T]^2}] \quad (2)$$

concentration in the stopped-flow spectrophotometer prior to dilution by one to one mixing.

Determination of Values for k_{cat} and k_{cat}/K_m. Because the K_m value of yeast ODCase for OMP is approximately 1−2 μM (*3*, *5*, *9*) and the maximal value of the change in extinction coefficient for decarboxylation of OMP is only 2.4 mM^{-1} cm^{-1}, it is difficult to measure the steady-state kinetic parameters for decarboxylation of OMP by this enzyme spectrophotometrically using initial velocity data. Consequently, analysis of the complete product curve was used herein to estimate the steady-state kinetic parameters. This method was usable because the product UMP is an ineffective inhibitor of the decarboxylation reaction (K_i > 200 μM, Table 1). In these experiments, the initial concentration of OMP was typically between 20 and 40 μM to obtain a good estimate of V_m. The end of the product curve was analyzed as a first-order process with a k_{obs} value that was approximately equal to V_m/K_m (eq 3).

$$v = -\frac{dS(t)}{dt} = -\frac{V_m[S(t)]}{[S(t)] + K_m} \quad (3a)$$

$$v = -\frac{V_m}{K_m}[S(t)] \text{ for } K_m > [S] \quad (3b)$$

$$P(t) = P_\infty(1 - e^{-V_m t/K_m}) \quad (3c)$$

To eliminate problems of time-dependent oligomerization, the standard buffer was used for these experiments. These data were collected with the stopped-flow spectrophotometer and were analyzed with the first-order fitting routine included with the instrument. The fit range was decreased until a constant value for k_{obs} was obtained. Values for k_{cat} and k_{cat}/K_m were calculated by dividing the values for V_m and V_m/K_m by $[E_T]$ respectively. K_m values were calculated from the ratio of k_{cat} to k_{cat}/K_m. For these experiments, the concentration of enzyme was always such that $[E_T]/2$ was less that 20% of the measured K_m value.

pH Dependence of k_{cat}/K_m, k_{cat} or k_1. Values of k_{cat}/K_m, k_{cat}, and the bimolecular association rate constants (k_1) of selected inhibitors were measured as a function of pH. The enzyme (0.5 μM) in 0.5 mM MOPS-Na^+, 100 mM NaCl, at pH 7.2 was loaded into one syringe of the stopped-flow spectrophotometer, whereas the other syringe contained 0.05 M buffer and 100 mM NaCl at the selected pH with the selected ligand. The buffers were acetate (pH 4−5.0), MES (pH 5.5−6), MOPS (pH 6.5−7.5), Tricine (pH 8.0−8.5), CHES (pH 9.05), and CAPS (pH 9.5−10.5). The bell shaped dependencies of k_{cat}/K_m on pH were described by two ionizing residues (Scheme 2). For brevity, this scheme assumes that both ionizations were associated with the enzyme. However, analogous equations were applicable if one ionization is associated with the enzyme and the other ionization is associated with the substrate. Equation 4 described the pH rate profile ($k([H^+])$ for this kinetic scheme where k is k_{cat}/K_m, k_{cat}, or k_1 for ligand binding. Values for

$$k([H^+]) = \frac{k}{\left(1 + \frac{[H^+]}{K_1} + \frac{K_2}{[H^+]}\right)} \quad (4)$$

k_{cat} and k_{cat}/K_m were determined as described above. Values for k_1 were calculated from data from the stopped-flow spectrophotometer that monitored the time courses of quenching of intrinsic protein fluorescence (λ_{ex} = 280 nm and λ_{em} > 320 nm) upon binding of the ligand to E_2. Typically, the pseudo first-order rate constant (k_{obs}) was determined at a single concentration of ligand (2−10 μM). The value of k_1 was calculated by dividing k_{obs} by the ligand concentration.

Titration of E_2 with OMP. The intrinsic protein fluorescence of E_2 was quenched transiently upon mixing enzyme with OMP. This fluorescence change was used to monitor the binding of E_2 to OMP. The stoichiometry for binding of OMP to E_2 was determined by titrating E_2 with OMP. Because the K_m of E_2 for OMP was significantly smaller in the absence of NaCl than in its presence and the goal of these experiments was to estimate the stoichiometry of OMP binding to E_2, the titration experiment was performed in the absence of added NaCl. The fluorescence change upon mixing 8.9 μM enzyme with an equal volume of selected concentrations of OMP was monitored with the stopped-flow spectrophotometer with λ_{ex} = 280 nm and λ_{em} > 320 nm. These data were analyzed for the case of n independent tight binding sites per monomeric enzyme (eq 5) where E_T was the concentration of enzyme expressed as monomer and K

Table 1: Parameters for Interaction of Selected Ligands with E_2 in the Presence of 100 mM NaCl[a]

ligand	K_i, μM	k_1, $\mu M^{-1} s^{-1}$	k_{-1}, s^{-1}	K_d, μM[b]	pK
OMP	na	62 (8)	60 (2)	1.0 (3)	6.38 (3)[c]
BMP	nd	100 (2)	nd	nd	nd
6-NH_2C(S)UMP	nd	7.9 (2)	0.00417 (3)	0.00052 (2)	8.7 (1)
6-AzaUMP	0.093 (3)	112 (5)	2.79 (4)	0.025 (1)	6.77 (8)
OxypurinolMP	0.052 (5)	nd	nd	nd	5.27 (6)
8-AzaXMP	0.12 (1)	130 (4)	11.7 (8)	0.09 (3)	4.5 (1)
AllopurinolMP	4.0 (4)	nd	nd	nd	8.93 (2)
ThiopurinolMP	2.5 (3)	24 (1)	30 (1)	1.2 (4)	7.66 (8)
XMP	24 (8)	nd	nd	nd	5.33 (4)
UMP	410 (5)	nd	nd	210 (2)[d]	9.7 (1) 6.26 (4)[c]
dUMP	nd	nd	nd	170 (2)[d]	nd
FdUMP	nd	nd	nd	250 (1)[d]	7.90 (9)
R-5-P	500 (1)	nd	nd	290 (2)[d]	6.25 (5)[c]

[a] K_i, k_1, k_{-1}, and pK values were determined as described in Experimental Procedures. [b] The K_d value was calculated from the ratio of the values for k_{-1} and k_1. [c] pK of phosphoryl group. [d] Calculated from data monitoring quenching of intrinsic protein fluorescence.

Scheme 2: Kinetically Important Protonation States of E_2

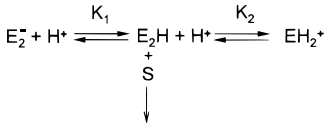

Scheme 3: Simple Kinetic Scheme for Decarboxylation of Orotidylate by E Assuming the Subunits of E_2 are Catalytically Independent

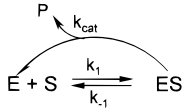

was the K_m of enzyme for OMP. The derivation of this expression is analogous to that described by Segal (*24*).

$$\Delta F([\mathrm{OMP}]) = \Delta F_\infty \left(\frac{1}{2n\mathrm{E_T}}\right)[(n\mathrm{E_T} + K + [\mathrm{OMP}]) - ((n\mathrm{E_T} + K + [\mathrm{OMP}])^2 - 4n\mathrm{E_T}[\mathrm{OMP}])^{0.5}] \quad (5)$$

Determination of Pre-Steady-State Parameters from Monitoring Changes in Intrinsic Protein Fluorescence upon Formation of E_2•S_2 or E_2•I_2. The intrinsic protein fluorescence of enzyme (0.2−10 μM) in the standard buffer was quenched upon formation of E_2•S_2. As OMP was decarboxylated the intrinsic fluorescence returned to that of resting enzyme. These changes were monitored with the stopped-flow spectrophotometer with $\lambda_{ex} = 280$ nm and $\lambda_{em} > 320$ nm. The approach to the steady-state upon mixing S with E_2 was analyzed by the simple mechanism of Scheme 3. The approach to the steady-state was described by a pseudo first-order process rate constant (k_{obs}). k_{obs} was related to the kinetic parameters of Scheme 3 by eq 6. From the slope of

$$k_{obs} = k_1[\mathrm{S}] + k_{-1} + k_{cat} \quad (6)$$

the plot of k_{obs} versus [S] the value of k_1 and the value of the sum of k_{-1} and k_{cat} were estimated. The value of k_{-1} was estimated from the value for k_{cat} and the value for the sum of k_{cat} and k_{-1}.

Changes in [H^+] during the Decarboxylation of OMP by E_2 in a Single Turnover Experiment. Small changes in the pH of a weakly buffering solution (0.5 mM MOPS Na^+, 100 mM NaCl at pH 7.2) were monitored by the fluorescence changes in 0.18 μM BCECF (pK = 7). With $\lambda_{ex} = 500$ nm and $\lambda_{em} > 520$ nm. Enzyme (25 μM) in 0.5 mM MOPS Na^+, 100 mM NaCl at pH 7.2 was mixed with an equal volume of 20 μM OMP in the stopped-flow spectrophotometer. The observed fluorescence changes were related to the change of [H^+] by independent experiments in which 10 μM HCl was added to the enzyme solution containing BCECF. The contribution of CO_2 to the observed pH changes was estimated by performing the reaction in the absence and presence of 2.5 μM carbonic anhydrase. A double exponential function (eq 7) or a single-exponential function ($\Delta F_2 = 0$) in eq 7 were fitted to the respective time courses.

$$\Delta F(t) = \Delta F_1 e^{-k_1 t} + \Delta F_2 e^{-k_2 t} + F_\infty \quad (7)$$

Determination of the Value of k_{-1} for Dissociation of E_2•I_2. The first-order rate constant describing the dissociation of E_2•I_2 was determined in a competition experiment. BMP is a high affinity inhibitor of E that we found did not quench the intrinsic protein fluorescence of E significantly (<5%), whereas the fluorescence of the protein was quenched significantly by 6-AzaUMP, 6-NH_2C(S)UMP, and ThiopurinolMP. Thus, addition of excess BMP to preformed complexes of E with these inhibitors (~1 μM) would result in a first-order increase of the intrinsic protein fluorescence E_2•I_2 to that of E•BMP. Demonstration that the observed rate constant was independent of BMP concentration used in the trapping experiments confirmed that the observed rate constant was for the dissociation of E_2•I_2. A single-exponential function was fitted to these data (eq 7 with $\Delta F_2 = 0$).

Determination of pK Values of Substrate Analogues. The ligands selected for these studies had pKs associated with the 5-phosphoribosyl moiety and the nucleobase moiety. Titration of the phosphoryl group was monitored potentiometrically. OMP, R-5-P, and UMP were titrated with HCl by this technique. The ligand (~20 mg of the Na^+ salt) was dissolved in 7 mL of 100 mM NaCl. The pH of the solution was recorded between additions of 2 μmol of HCl at room temperature (~24 °C). Equation 8 was fitted to the titration data where A was the micromoles of HCl required for titration of the group, A([H^+]) was the number of micromoles of HCl required for this [H^+], K was the dissociation constant of the group being titrated, and C was zero.

$$A([\mathrm{H^+}]) = \frac{A[\mathrm{H^+}]}{([\mathrm{H^+}] + K)} + C \quad (8)$$

The nucleobase moieties of the substrate analogues were titrated spectrophotometrically. The wavelengths used for monitoring these titrations were 235 nm for 6-NH_2C(S)UMP, 243 nm for 6-AzaUMP, 280 nm for 8-AzaXMP, 271 nm for OxypurinolMP, 321 nm for ThiopurinolMP, 271 nm for AllopurinolMP, 281 nm for XMP, 229 nm for FdUMP, and 261 nm for UMP. The absorbsance of a ~200 μM solution of these analogues was measured at 25 °C in the same pH buffers used for the determination of the pH dependence of k_{cat}/K_m. Equation 8 was fitted to these data where $A([H^+])$ was the absorbance at $[H^+]$, A was the maximal absorbance change, K was the dissociation constant of the group on the nucleobase, and C was the absorbance for $[H^+] = 0$.

Determination of the Kinetic Parameters for Interaction of 8-AxaXMP with E_2. In contrast to the other substrate analogues of OMP investigated herein, 8-AxaXMP was highly fluorescent (λ_{ex} = 285 nm, λ_{em} > 320 nm). The fluorescence of 8-AzaXMP was enhanced upon binding to E_2. Consequently, the change in fluorescence upon binding 8-AzaXMP to the enzyme was a combination of the quenching of intrinsic protein fluorescence and the increase in the fluorescence of 8-AzaXMP. Consequently, experiments monitoring the binding of 8-AzaXMP to the enzyme were limited to conditions in which the enzyme concentration (~5 μM) was greater than the concentration of 8-AzaXMP. Under these conditions, the pseudo first-order rate constant for the reaction of 8-AxaXMP with enzyme describe a reaction that was first-order in 8-AxaXMP.

Determination of K_i Values of E_2 for Selected Substrate Analogues. The K_i values for selected substrate analogues were estimated from the effect that the selected analogue had on the K_m of E_2 for OMP. The dependence of the apparent K_m on the concentration of analogue ([I]) was described by eq 9. Several analogues were tested at multiple

$$K_m^{app} = K_m\left(1 + \frac{[I]}{K_i}\right) \quad (9)$$

concentrations to confirm the relation of eq 9, which indicated analogues were competitive inhibitors. Most analogues were tested at a single concentration.

Determination of the Bimolecular Association Rate Constant for Association of E_2 with BMP. The formation of E_2•BMP_2 was not associated with a significant change in the intrinsic protein fluorescence. Consequently, a competitive method was used to estimate the bimolecular rate constant for association of E_2 and BMP. Formation of E_2•6-NH_2C(S)UMP_2 was associated with a large change in the intrinsic protein fluorescence that could be monitored spectrofluorometrically. Thus, the pseudo first-order rate constant for binding of E_2 to 6-NH_2C(S)UMP was determined as a function of BMP concentration. The amplitude of the reaction decreased as the concentration of BMP was increased at a fixed concentration of 6-NH_2C(S)UMP. This was consistent with the two ligands competing for the same site. The dependence of the pseudo first-order rate constant (k_{obs}) for the fluorescence decrease on the concentration of BMP was given by eq 10 where k_0 was the value of k_{obs} in the absence of added OMP and k_1 was the bimolecular association rate constant of E_2 and OMP.

$$k_{obs} = k_1[BMP] + k_0 \quad (10)$$

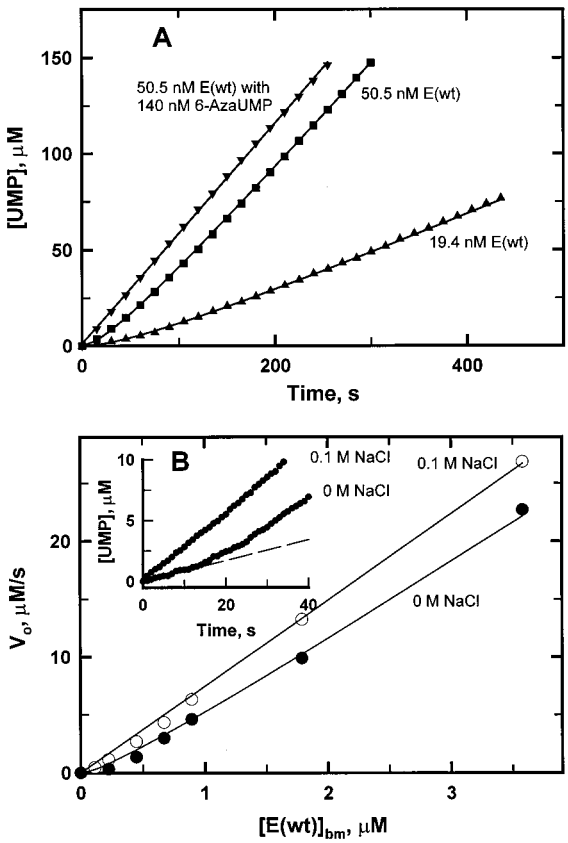

FIGURE 1: Substrate-dependent activation of diluted ODCase. Panel A, E (5.2 μM) was prepared in 0.01 M MOPS-Na^+, 100 mM NaCl at pH 7.2 and room temperature. The enzyme was diluted 100- or 250-fold into 0.01 M MOPS-Na^+ and 0.21 mg/mL bovine serum at pH 7.2 and 25 °C to give final enzyme concentrations of 50.5 and 19.4 nM. The reaction was initiated 45 s after dilution with 160 μM OMP. Equation 1 was fitted to these time courses to give k_{cat} = 11.26 (5) s^{-1} and k = 1.56 (4) μM^{-1} s^{-1}. If the enzyme was diluted into 140 nM 6-azaUMP [K_i = 25 nM (Table 1)] prior to addition of OMP (leftmost tracing), the rate of UMP formation was constant over the observation interval. Panel B, effect of enzyme concentration on the initial velocity of OMP decarboxylation in the presence and absence of 100 mM NaCl. Enzyme at the indicated concentrations (before mixing) was equilibrated in the stopped-flow spectrofluorometer for 2 min in 0.01 M MOPS-Na^+ with or without 100 mM NaCl. The equilibrated enzyme solution was mixed with an equal volume of 92 μM OMP. The value of the initial velocity was assumed to be proportional to the active dimer concentration immediately after mixing equilibrated ODCase with OMP (main figure). Equation 2 was fitted to these data to give k_{cat} = 14.9 (2) s^{-1} and K = 0.25 (5) μM.

RESULTS

Ligand Induced Enzyme Dimerization. The initial velocity of OMP decarboxylation in 0.01 M MOPS pH 7.2 was highly dependent on whether the reaction was initiated with OMP or with enzyme. For example, if the reaction was initiated by the addition of 50.5 nM enzyme from a 2 μM stock solution into 160 μM OMP, the time course of product formation was linear. In contrast, if 19.4 or 50.5 nM enzyme were equilibrated for 60 s in this buffer prior to addition of OMP, the velocity of the reaction increased from a value that was essentially zero to that observed for a reaction initiated with enzyme (Figure 1A). The magnitude of the lag in UMP formation was dependent on the length of time that enzyme was preincubated in buffer prior to addition of OMP. Preincubation of enzyme for 5 s prior to addition of substrate

resulted in an insignificant lag in UMP formation, whereas 30 and 120 s preincubations yielded significant lags of comparable amplitudes. Bovine serum albumin at 0.21 mg/mL, which was included to minimize absorption of the enzyme to the cuvette, did not affect the time course of UMP formation. These data demonstrated that substrate induced an oligomerization of the enzyme from an inactive to an active form as described by Scheme 1. This mechanism assumed that (i) monomeric enzyme did not bind substrate, (ii) the dimeric form of the enzyme was the catalytically active species, and (iii) the concentration of free E_2 was insignificant at the substrate concentration used for these experiments, i.e., [OMP] $\gg K_m$ such that dimer formation is functionally irreversible. Equation 1 describes the time-dependent decarboxylation of OMP by enzyme that was initially in the monomeric state. Because the concentration of E_2 was assumed to be very small ([OMP] $\gg K_m$, assumption 3), eq 1 does not include a contribution from k_r. Equation 1 with $k_{cat} = 11.26$ (5) s^{-1} and $k_f = 1.56$ (4) μM^{-1} s^{-1} accurately described the time course for decarboxylation of OMP at the two enzyme concentrations tested. This finding indicated that the enzyme dimer, not a higher order oligomer, was the catalytically active species.

If 50.5 nM enzyme was pre-equilibrated for 45 s in buffer containing 100 mM NaCl prior to addition of OMP, the time course for UMP formation was linear. Furthermore, if 50.5 nM enzyme was pre-equilibrated for 45 s in buffer containing 140 nM 6-AzaUMP, a potent competitive inhibitor of the decarboxylation reaction with a $K_i = 25$ nM (Table 1), the time course for UMP formation was also linear (Figure 1). These results suggested that NaCl and 6-AzaUMP stabilize the catalytically active dimeric enzyme.

An estimate for the value of the bimolecular rate constant for association of E (k_f) was made from the above results. The system would be completely described with an estimation of either a value for the first-order rate constant describing the dissociation of E_2 or a value for the overall equilibrium constant for dimer dissociation (K). An estimate of the dimer dissociation constant was made from the concentration dependence of E_2 on total enzyme concentration. The concentration of E_2 in these mixtures was calculated from the initial velocity of OMP decarboxylation. Because dimerization was rapid, initial velocity data were collected with the stopped-flow spectrophotometer (Figure 1B, inset). Solutions of selected concentration of enzyme were pre-equilibrated for 120 s prior to mixing with an equal volume of 92 μM OMP. The buffer was 0.01 M MOPS-Na^+, pH 7.2, in the presence or absence of 100 mM NaCl. In the presence of 100 mM NaCl, the velocity of UMP formation was linearly dependent on enzyme concentration. However, the initial velocity for decarboxylation of OMP by 0.32 μM enzyme increased 3-fold as the concentration of NaCl was increased from 0 to 150 mM. The concentration of NaCl that gave 50% of the maximal effect was 6 mM. In the absence of NaCl, the initial velocity of OMP decarboxylation was nonlinearly dependent on enzyme concentration (Figure 1B). Equation 2, derived for the mechanism of Scheme 1, describes the dependence of the initial velocity of OMP decarboxylation on the concentration of enzyme. The fit of eq 2 to the data of Figure 1B yielded a $k_{cat} = 14.9$ (2) s^{-1} and a $K = 0.25$ (5) μM. The value of k_r in Scheme 1 was calculated from the values of K and k_f to be 0.16 s^{-1}.

A pivotal assumption for the derivations of eqs 1 and 2 was that the affinity of monomeric enzyme for OMP was much less than that of dimeric enzyme. In agreement with this assumption was the observation that 6-NH_2C(S)UMP, a potent inhibitor of the enzyme (*25*), rapidly quenched the intrinsic protein fluorescence (~50%) at high enzyme concentration but only slowly quenched the protein fluorescence at low enzyme concentration. Furthermore, 6-NH_2C(S)UMP rapidly quenched the fluorescence of 0.25 μM enzyme in a monophasic reaction in the presence of 100 mM NaCl (conditions for which the enzyme was essentially a dimer). This reaction was biphasic in the absence of NaCl (conditions for which the enzyme was a mixture of monomer and dimer). In the latter reaction, the early phase was assigned to dimeric enzyme binding inhibitor, whereas the late phase was assigned to monomeric enzyme dimerizing prior to inhibitor binding. An equation analogous to eq 2 was derived to describe the concentration dependence of the amplitude of the early phase (dimer concentration) on total enzyme concentration. The value of the dimerization constant estimated from these data was 0.23 (1) μM. The time course of the late phase of the quenching reaction was similar to that for the onset of catalytic activity (Figure 1A). The value of the forward rate constant for dimerization (k_f) was estimated from the late phase of the inhibitor binding reaction to be 2.0 (5) μM^{-1} s^{-1}. These values for k_f and K estimated from data monitoring the binding of 6-NH_2C(S)UMP to enzyme were similar to those estimated from initial velocity data and time course of OMP decarboxylation data described above. Because 6-NH2C(S)UMP did not quench the fluorescence of monomeric enzyme significantly, the monomeric enzyme probably did not bind the ligand. Attempts to measure subunit dimerization directly by monitoring changes in protein fluorescence were unsuccessful.

To avoid problems introduced by the time-dependent dimerization of the enzyme, all subsequent experiments were performed in the presence of 100 mM NaCl. Under these conditions, the enzyme was essentially in the dimeric form.

Steady-State Kinetic Parameters for Decarboxylation of OMP. The values of k_{cat} and K_m were determined from the complete time course for decarboxylation of OMP (Figure 2A). Values for V_m and V_m/k_{cat} were calculated from the initial and final phases of the reaction, respectively. The k_{cat} and K_m values for OMP were 14.1 (1) s^{-1} and 1.65 (6) μM, respectively. Values for these parameters from independent experiments ranged between 13 and 16 s^{-1} for k_{cat} and between 1.5 and 2 μM for K_m. The value of the K_m for the reaction was very dependent on the NaCl concentration. With NaCl concentrations of 0.05, 0.1, 0.2, and 0.3 M, the K_m values were 0.53, 1.6, 5.0, and 10.0 μM, respectively. NaCl did not affect the value of k_{cat} significantly.

The pH dependence of k_{cat}/K_m (Figure 2B) was bell-shaped, which indicated two ionizations in free enzyme or substrate that were important for binding. Equation 4 was fitted to these data to give pK values of 6.1 (1) and 7.7 (1). The pH independent value of k_{cat}/K_m was 11 (1) μM^{-1} s^{-1}. The pH dependence of k_{cat} was also bell-shaped (Figure 2B). Equation 4 was fitted to these data to give pK values of 4.66 (8) and 8.84 (8) with a pH independent value for k_{cat} of 14.4 (4) s^{-1}.

Pre-Steady-State Kinetic Analysis of the Interaction of OMP with E_2. Catalytically active enzyme was a dimer (E_2). To demonstrate that both active sites of E_2 simultaneously

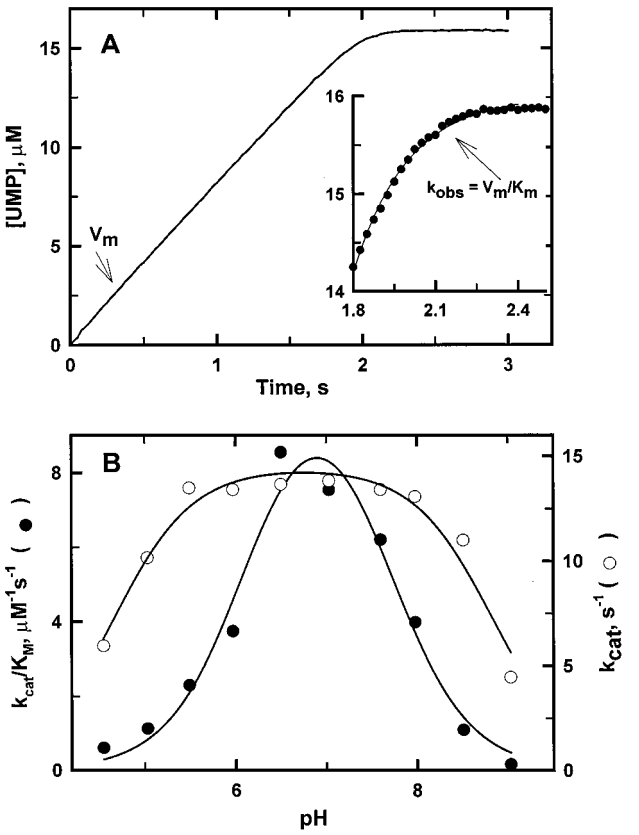

FIGURE 2: Kinetic parameters for the decarboxylation of OMP by E_2. The decarboxylation of 16 μM OMP by 0.6 μM E_2 in the presence of 100 mM NaCl was monitored spectrophotometrically. Panel A, the maximal velocity (V_m) was calculated from the data of the main figure to be 8.46 (2) μM s^{-1}. The value of V_m/K_m was calculated to be 5.1 (2) s^{-1} from the time dependence of the end of the reaction (formation of ~1 μM product) as described by eq 3c (inset). Panel B, pH dependence of k_{cat} and k_{cat}/K_m. The concentration of E_2 was 0.5 μM and the initial concentration of OMP was 20 μM. The time course data was analyzed as described in panel A. Equation 4 was fitted to the k_{cat}/K_m data to give pK_1 = 6.1 (1), pK_2 = 7.7 (1), and a pH-independent value of k_{cat}/K_m = 8.0 (8) μM^{-1} s^{-1}. Equation 4 was fitted to the k_{cat} data to give pK_1 = 4.66 (8), pK_2 = 8.84 (8), and a pH-independent value of k_{cat} = 14.4 (4) s^{-1}.

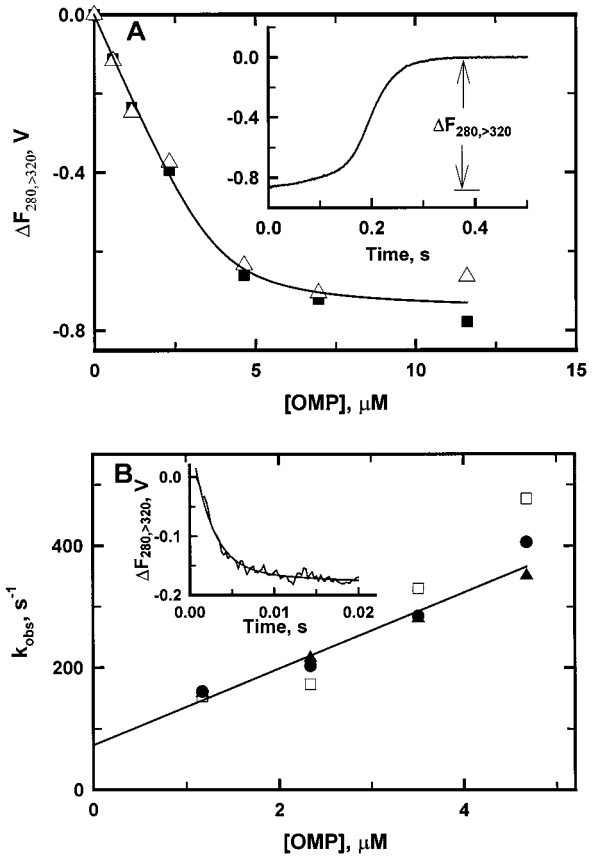

FIGURE 3: Quenching of intrinsic protein fluorescence of E_2 by OMP. Panel A, titration of intrinsic protein fluorescence by OMP. The fluorescence of the E (10 μM) is rapidly quenched (not time-resolved in this experiment) upon mixing with 40 μM OMP in the standard buffer (inset). After depletion of OMP the fluorescence returns to that of untreated E. The amplitude of the fluorescence change ($\Delta F_{280,>320}$) with 4.45 μM E_2 was determined in two independent experiments (open triangles and closed squares) as a function of OMP concentration in 0.01 M MOPS pH 7.2. These data were fitted to eq 5 to give n = 0.85 (7), ΔF_∞ = −0.75 (3), and K = 0.2(2) μM. Panel B, dependence of the rate constant describing the approach to the steady-state on the concentration of OMP. The approach to the steady-state upon reacting 0.43 μM E_2 with 4.7 μM OMP (inset) is a first-order process described by a pseudo first-order rate constant of 410 (1) s^{-1}. The dependence of the value of this rate constant on OMP concentration (main figure) was described by eq 6 with $k_{cat} + k_2$ = 70 (2) s^{-1} and k_1 = 62 (7) μM^{-1} s^{-1}.

bound substrate (i.e., the enzyme did not exhibit half-site reactivity), the stoichiometry between substrate and E_2 was determined by monitoring the large changes in the intrinsic protein fluorescence occurring during the decarboxylation of OMP by E_2 (Figure 3A, inset). The fluorescence of E_2 was rapidly quenched to a steady-state level upon addition of 40 μM OMP to 10 μM E_2 (not time-resolved in the inset to Figure 3A). The fluorescence of the enzyme returned to that of resting enzyme upon substrate depletion. This change in enzyme fluorescence was titrated with OMP in the absence of NaCl (Figure 3A, main figure). These conditions were chosen to obtain a robust estimate for the stoichiometry of E_2 for OMP; an estimate from this experiment of the affinity for the enzyme for OMP was of secondary importance. Decreasing the NaCl concentration from the concentration in the standard buffer (100 mM to 0 M) decreased the K_m of the enzyme for OMP from a value of 1.6 μM to less than 0.1 μM. The enzyme concentration (4.45 μM) was sufficiently high in these experiments that NaCl could be eliminated from the buffer without increasing the concentration of monomeric enzyme significantly. Equation 5 was fitted to these data to give a value for n of 0.85 (7), where n was the number of OMP binding sites per monomer. Thus, the stoichiometry for binding of OMP to E_2 was one substrate per monomer enzyme. The stoichiometry for binding of 6-NH_2C(S)UMP to the enzyme was found to be 0.85 per enzyme monomer. Thus, each subunit of the dimeric enzyme simultaneously bound ligand with comparable affinities.

The reaction of E_2 with OMP to yield the enzyme−substrate complex with reduced intrinsic protein fluorescence (time-resolved in inset to Figure 3B) was a first-order process. Even though the time-resolved portion of the reaction did not deviate significantly from a first-order process, over 50% of the fluorescence change was completed within the dead time (1.8 ms) of the stopped-flow spectrophotometer. Nonetheless, the extent of the missed reaction was consistent with the value of the observed pseudo first-order rate constant describing the time-resolved portion of the reaction and the dead-time of the instrument. These

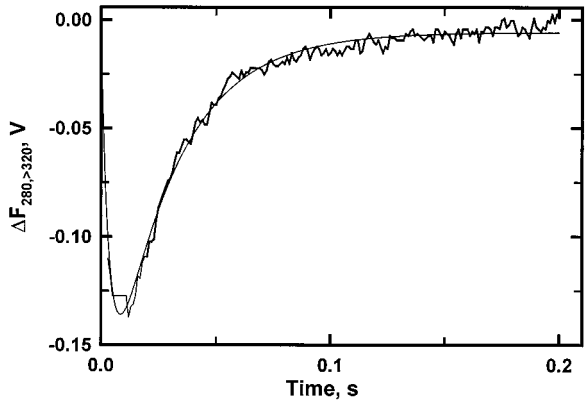

FIGURE 4: Single turnover of E with OMP. The reaction of 6.8 μM E_2 with 0.5 μM OMP was monitored by the changes in intrinsic protein fluorescence. Equation 7 was fitted to these data with ΔF_1 equal to $-\Delta F_2$ to give $k_1 = 270$ (1) s^{-1}, $k_2 = 36.6$ (7) s^{-1}, $\Delta F_1 = 0.205$ (4), and $\Delta F_\infty = -0.0057$ (4).

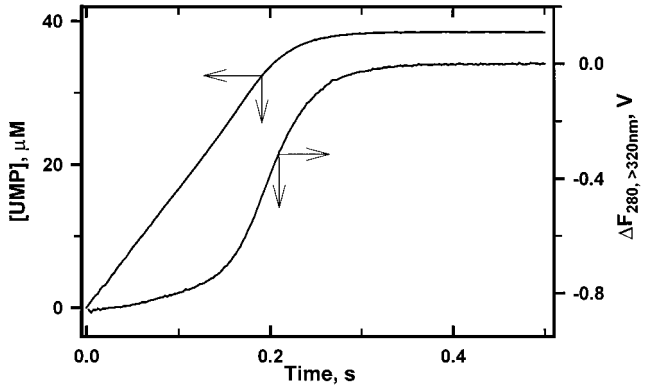

FIGURE 5: Correlation of UMP formation with changes in intrinsic protein fluorescence during the decarboxylation of OMP by E_2. The reaction of 10 μM E with 40 μM OMP in the standard buffer was monitored by the absorbance changes associated with UMP formation (A_{279}) and by the changes in intrinsic protein fluorescence ($F_{280,>320}$).

results were consistent with E_2 functioning as a single species in its reaction with OMP, i.e., the two substrate binding sites on E_2 were functioning independently. The pseudo first-order rate constants describing the approach to the steady-state were linearly dependent on OMP concentration (Figure 3B, main tracing). These results were described by the mechanism of Scheme 3 in which E_2S_2 was the single time-resolvable intermediate on the catalytic pathway for decarboxylation of OMP. Equation 6 was fitted to these data to give $k_1 = 62$ (8) μM^{-1} s^{-1} and the sum of k_{-1} and $k_{cat} = 70(2)$ s^{-1}. The value of k_{-1} was calculated to be 60 (2) s^{-1} from this latter value and the value of k_{cat} (15 s^{-1}). The commitment to catalysis [$k_{cat}/(k_{-1})$] was calculated to be 0.25.

Because an enzymatic species with reduced fluorescence accumulated during OMP decarboxylation by E_2, the rate-limiting step of the reaction must occur after formation of this species. To estimate the rate of conversion of this species to the subsequent fluorescence species, a single turnover experiment was performed with $[E_2] \gg [S]$. Changes in intrinsic protein fluorescence were monitored during the reaction of 0.5 μM OMP with 6.8 μM enzyme in the standard buffer (Figure 4). Most of the early phase of the reaction corresponding to formation of the ES complex was not observed with the stopped-flow spectrophotometer. The disappearance of the species with reduced fluorescence was described by a first-order rate constant with a value of 36.4 (7) s^{-1}. If the conversion of the species with reduced fluorescence to the fluorescence species was the rate-determining step, the value measured in the single turnover experiment should approximate the value of k_{cat}. This value was similar to that measured for k_{cat} (15 s^{-1}).

If conversion of a species with fluorescence similar to that of resting enzyme occurred in the rate-determining step, an overshoot in the concentration of enzyme with reduced fluorescence should occur. Clearly from the data of Figure 5 there was no detectable overshoot in the concentration of the species with reduced fluorescence. These results suggested that no enzymatic species with the fluorescence of resting enzyme accumulated in the steady-state. Finally, UMP formation did not occur with a burst or lag (Figure 5) that suggested that UMP was released from the enzyme during the conversion of the enzyme species with reduced fluorescence to resting enzyme. Consequently, the simple kinetic mechanism of Scheme 3 adequately describes the OMP decarboxylation by E_2.

Changes in [H^+] during Decarboxylation of OMP in a Single Turnover Experiment. The previous experiment identified UMP formation as occurring during the conversion of the enzymatic species with reduced fluorescence to the species with the fluorescence of resting enzyme. The chemical nature and the order of release of the other reaction product from the enzyme were determined by monitoring pH changes during decarboxylation and by monitoring the effects of carbonic anhydrase on these pH changes. The pH changes were monitored with a fluorescent pH indicator (BCECF) in a weakly buffered solution (0.5 mM MOPS Na^+ with 100 mM NaCl at pH 7.2). The fluorescence change was related to a change in [H^+] as described in Experimental Procedures. The reaction of 12.5 μM E_2 with 10 μM OMP resulted in the transient consumption of 10.6 (1) μM hydrogen ions described by a first-order rate constant with a value of 21.3 (5) s^{-1} (Figure 6A). The consumption of hydrogen ions was correlated with the conversion of the enzyme species with reduced fluorescence to that with the fluorescence of resting enzyme [27 (2) s^{-1}, Figure 6A (inset)]. The pH of the reaction mixture returned to the starting value in a process described by a first-order rate constant with a value of 0.0375 (5) s^{-1} (Figure 6B).

If these measurements were repeated in the presence of 2.5 μM carbonic anhydrase, the associated changes in [H^+] were greatly reduced. Similar results were observed with 1.0 μM carbonic anhydrase. These results demonstrated that a proton was consumed with the release of CO_2 during the conversion of the enzyme species with reduced fluorescence to the species with the fluorescence of resting enzyme. The finding that the pH changes were not completely abrogated by the inclusion of carbonic anhydrase suggested that a fraction of the proton uptake was associated with changes in the protonation of the enzyme in the enzyme−substrate complex versus that in free enzyme.

Ligand Binding to E_2. The binding of selected substrate analogues (I) to E_2 was monitored by the changes in intrinsic protein fluorescence upon formation of $E_2 \bullet I_2$. The interaction of the competitive inhibitor 6-AzaUMP with E_2 was described by a pseudo first-order rate constant (Figure 7A,

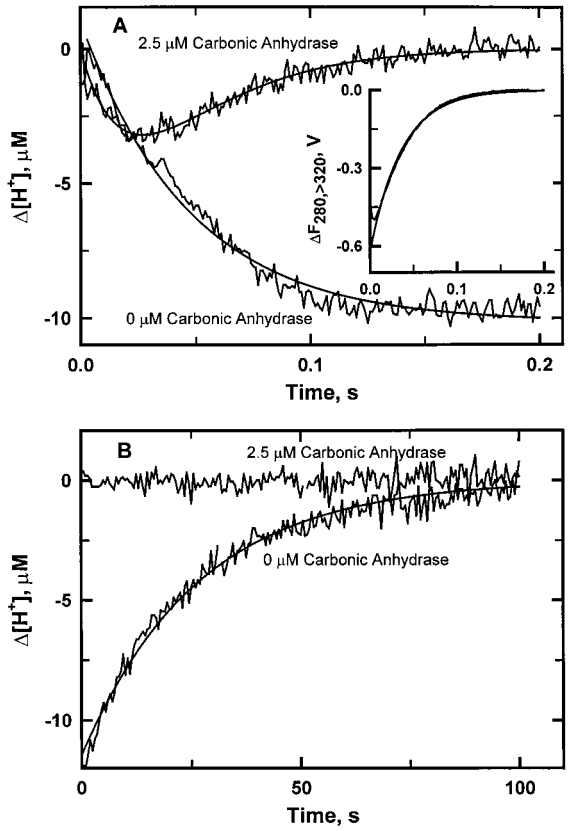

FIGURE 6: Kinetics of H^+ uptake and release during the decarboxylation of OMP by E_2. Changes in pH of the buffer (0.5 mM MOPS Na^+, 100 mM NaCl at pH 7.2) were monitored by the pH-dependent fluorescence of 0.18 μM BCECF (λ_{ex} = 500 nm, λ_{em} > 530 nm). Panel A, early time course for changes in H^+ concentration during the reaction of 12.5 μM E_2 with 10 μM OMP in the absence or presence of 2.5 μM carbonic anhydrase. In the absence of carbonic anhydrase, eq 7 was fitted to the data with $\Delta F_2 = 0$ to give $k_1 = 21.3$ (5) s^{-1}, $\Delta F_\infty = -10.16$ (6) μM, and $\Delta F_1 = 11.2$ (1) μM. In the presence of 2.5 μM carbonic anhydrase, eq 7 was fitted to the data with $\Delta F_1 = -\Delta F_2$ and $\Delta F_\infty = 0$ to give $k_1 = 44$ (9) s^{-1}, $k_2 = 31$ (5) s^{-1}, and $\Delta F_1 = 30$ (3) μM. The time course for the protein fluorescence changes in the presence of 0.18 μM BCECF was described by a first-order rate constant of 27 (2) s^{-1} (inset). Panel B, late time course for changes in H^+ concentration for the reactions described in panel A. In the presence of 2.5 μM carbonic anhydrase, eq 7 was fitted to the data with $\Delta F_1 = 0$ and $\Delta F_\infty = 0$ to give $k_1 = 0.0375$ (5) s^{-1} and $\Delta F_1 = -11.5$ (1) μM.

inset). The value of this pseudo first-order rate constant was linearly dependent on the concentration of 6-azaUMP. Equation 6 was fitted to these data ($k_{cat} = 0$) to yield k_1 = 112 (5) μM^{-1} s^{-1}. Similar determinations were made for 6-NH_2C(S)UMP, 8-AzaXMP, and ThiopurinolMP. Because BMP did not quench the fluorescence of E_2 significantly, the value of k_1 for this inhibitor was estimated by a competition experiment with NH_2C(S)UMP as described in Experimental Procedures. The results from these ligand-binding studies are summarized in Table 1.

pH Dependence of the Bimolecular Association Rate Constants for the Reaction of E_2 with Selected Analogues (k_1). The pH dependence of k_1 was determined for 6-AzaUMP (Figure 7B). Equation 4 was fitted to these data to give pK_1 = 6.6 (2), pK_2 = 8.0 (2), and a pH-independent k_1 = 130 (2) μM^{-1} s^{-1}. Similar determinations were made with 6-NH_2C(S)UMP and 8-AzaUMP. These results are summarized in Table 2.

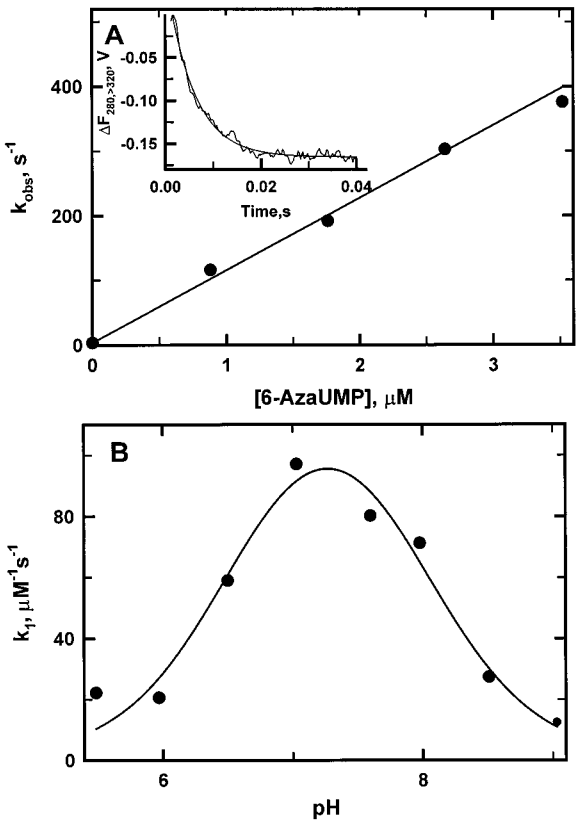

FIGURE 7: Kinetics for association of E_2 with 6-AzaUMP. Panel A, concentration dependence of the pseudo first-order rate constant describing the association of 6-AzaUMP with E. The reaction of 0.62 μM E_2 with 1.8 μM 6-AzaUMP was described by a first-order rate constant of 181 (3) s^{-1}. The value of this rate constant was linearly dependent on 6-AzaUMP concentration (main figure). The slope of this line (k_1) had a value of 112 (5) μM^{-1} s^{-1}. Panel B, pH dependence of the association rate constant for E_2 with 6-azaUMP (k_1). The dependence of the association rate constant on pH was described by eq 4 with k_1 substituting for k_{cat}. Equation 4 was fitted to these data to give k_1 = 130 (2) μM^{-1} s^{-1}, pK_1 = 6.6 (2), and pK_2 = 8.0 (2).

Table 2: pH Dependence of the Apparent Association Rate Constants (k_1 or k_{cat}/K_m) for E_2 and Selected Ligands

ligand	pK_1	pK_2	k_1 or (k_{cat}/K_m), μM^{-1} s^{-1}
OMP	6.1 (1)	7.7 (1)	11 (1)
6-NH_2C(S)UMP	5.8 (1)	8.79 (9)	7.7 (3)
6-AzaUMP	6.6 (2)	8.0 (2)	130 (2)
8-AzaXMP	5.3 (1)	8.2 (1)	81 (5)

Dissociation of E_2•6-AzaUMP$_2$. The intrinsic protein fluorescence of E_2•6-AzaUMP$_2$ was reduced relative to that of E_2•BMP$_2$. Consequently, the fluorescence change associated with the dissociation of E_2•6-AzaUMP$_2$ in the presence of excess BMP to form E_2•BMP$_2$ was a convenient method for monitoring the ligand exchange reaction (Figure 8). Because the observed rate constant was similar with two concentrations of BMP, it was assigned to the dissociation of E_2•6-AzaUMP$_2$. The dissociation rate constants for E_2•NH_2C(S)UMP$_2$, E_2•8-AzaXMP$_2$, and E_2•ThiopurinolMP$_2$ were determined in a similar manner (Table 1).

Effect of NaCl Concentration on the Association and Dissociation Rate Constants of E_2 for Selected Analogues. NaCl had a pronounced effect on enzymatic activity that was reflected in changes in the values of the dimerization constant and the K_m. Consequently, the effects of NaCl on the

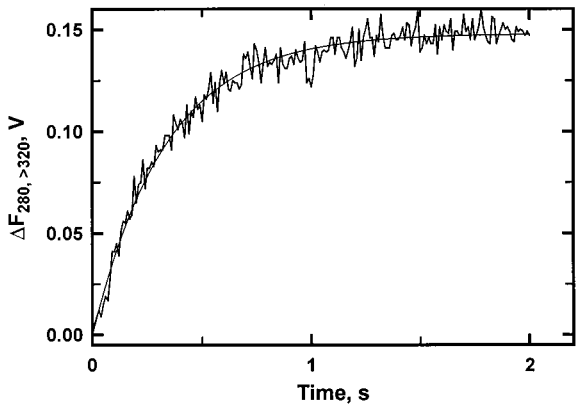

FIGURE 8: Kinetics of dissociation of E_2•6-AzaUMP$_2$. E_2•6-AzaUMP$_2$ was formed by equilibration of 1.24 μM E_2 with 1.28 μM 6-azaUMP for 5 min in the standard buffer. This solution was mixed with an equal volume of 2 μM BMP. Formation of E_2•BMP$_2$ was monitored by the increase in intrinsic protein fluorescence as E_2•6-AzaUMP$_2$ dissociated and E_2•BMP$_2$ formed. The reaction was described by a first-rate rate constant with a value of 2.78 (7) s^{-1}. The value of the first-order rate constant was similar with 8 μM BMP [3.43 (4) s^{-1}].

Table 3: Effect of NaCl on the Dissociation Rate Constants (k_{-1}, s^{-1}) and Association Rate Constants (k_1, μM^{-1} s^{-1}) for E_2 with Selected Ligands

[NaCl], M	6-AzaUMP	6-NH_2C(S)UMP	OMP
	k_{-1}, s^{-1}	k_{-1}, s^{-1}	k_{-1}, s^{-1}
0	0.84 (1)	0.00105 (8)	nd
0.1	2.79 (4)	0.00417 (3)	60 (2)
	k_1, μM^{-1} s^{-1}	k_1, μM^{-1} s^{-1}	k_1, μM^{-1} s^{-1}
0	700 (1)	37 (2)	>300
0.1	112 (5)	7.9 (4)	62 (8)

association rate constants and the dissociation rate constants of E_2 for selected ligands were determined. The concentration of enzyme in these experiments was sufficiently high that it was present as E_2 in the absence of NaCl. The results with OMP, 6-AzaUMP, and 6-NH_2C(S)UMP are summarized in Table 3.

DISCUSSION

In contrast to the bifunctional uridine 5′-phosphate synthase from mammal sources that contains both ODCase and phosphoribosyltransferase activities (*18*), yeast ODCase is a monofunctional protein that lacks the phosphoribosyltransferase activity (*9*). This greatly simplifies mechanism studies. Nonetheless, the state of oligomerization of the yeast enzyme is dependent on the presence of allosteric effectors (*9*, *18*). Sedimentation studies demonstrated that the enzyme was in a monomer−dimer equilibrium (*9*, *18*). Recent X-ray crystallographic studies demonstrated that the yeast enzyme crystallized as the dimer both in the absence and presence of ligand (*19*). As a prelude to our kinetic analysis of yeast ODCase, the rate at which the monomer−dimer equilibrium was established and an estimate of the dimerization constant were determined. Surprisingly, the attainment of the monomer−dimer equilibrium was very rapid ($t_{1/2}$ < 10 s with 50 nM enzyme). Mammalian uridine 5′-phosphate synthase, which has ODCase activity, also undergoes a rapid monomer−dimer equilibration in the presence of OMP (*26*). The dimer dissociation constant for the yeast enzyme was 0.25 μM in 0.01 M MOPS Na^+ at pH 7.2. Formation of E_2 was favored

Scheme 4: Expansion of Scheme 3 Describing the Decarboxylation of Orotidylate by E_2

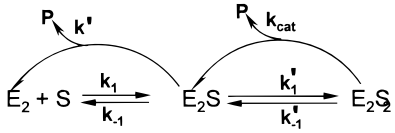

by the inclusion of NaCl in the buffer. Concomitant with the shift in the monomer−dimer equilibrium, NaCl increased the K_m of the enzyme for OMP significantly. The value of the K_m was 1.5 μM in the presence of 100 mM NaCl, whereas the value of this parameter appeared to extrapolate to a value less than 0.1 μM as the NaCl concentration was decreased to zero. The mechanism by which NaCl decreased the affinity of OMP for the enzyme was more than simply Na^+ or Cl^- competing for the OMP binding site. The association rate constant for the substrate analogue, 6-AzaUMP, was 7-fold greater in the absence of added NaCl than in the presence of 100 mM NaCl. This observation might appear consistent with a simple competition between ligand and Na^+ or Cl^- for a common site on the enzyme. However, the dissociation rate constants of E_2•6AzaUMP$_2$ and E_2•6-NH_2C(S)UMP$_2$ were 3- to 4-fold larger in the presence of 100 mM NaCl than in its absence (Table 3). If these salt effects were only the result of competition for the ligand-binding site, the dissociation rate constant for E_2•I_2 should have been independent of NaCl. These results suggested that the salt effects involve interactions at sites other than the ligand-binding site. To eliminate complications in our kinetic studies resulting from the time-dependent monomer−dimer equilibration of the enzyme, 100 mM NaCl was included in the standard buffer. Under these conditions, kinetic studies suggested that the enzyme was in the dimeric state at protein concentrations as low as 5.0 nM. With yeast ODCase, monomer formation is probably an artifact of the in vitro assay system. In the yeast cell, ODCase has been estimated to be between 260 and 375 nM (*18*). With the cellular salt concentration and this enzyme concentration, the enzyme would be present essentially as the dimer.

Because the enzyme was a dimer under the conditions of our assay, two potentially nonequivalent ligand-binding sites exist as described by Scheme 4. The crystal structure of the yeast enzyme ligated with BMP revealed that the active site of each subunit of the dimeric enzyme was fully occupied by ligand (*19*). Similar results were observed in the X-ray structures of enzyme from *M. thermoautotrophicum* and *B. subtilis* ligated with 6-AzaUMP and UMP, respectively (*20*, *21*). If, however, the binding of the substrate to the enzyme exhibited negative cooperativity, only one of these sites might be catalytically active and the stoichiometry of substrate binding would be 0.5 mol of substrate per mole of monomer. The titration of the enzyme with substrate showed that 0.85 mol of substrate was bound per mole of monomer. This result indicated that both subunits bound substrate with comparable affinities. The effect of active site occupancy on k_{cat} was estimated by comparison of the steady-state value of k_{cat}, which was obtained by extrapolation to infinite substrate, to the value of k' in which a single subunit was occupied by substrate (Scheme 4). The value of k' was derived from a single turnover experiment ([S] ≪ [E]) in which the first-order rate for disappearance of a spectrofluorometrically

competent intermediate in catalysis was determined. The value of k_{cat} was typically 14−16 s^{-1}, whereas the disappearance of the kinetically competent intermediate (k') was 36 s^{-1}. The value of k_{cat} was dependent on accurate estimates of enzyme concentration and $\Delta\epsilon_{279}$ for product formation, whereas the value of k' was independent of an accurate determination of enzyme and OMP concentrations. In view of the errors associated with the values for active enzyme concentration and $\Delta\epsilon_{279}$, it is not unreasonable to propose that the observed values for k_{cat} and k' are similar, if not equivalent. Thus, each monomer of the dimeric enzyme functions independently even though crystallographic data identified subunit−subunit interactions upon formation of the catalytically competent enzyme (*19*).

The kinetic characterization of subunit oligomerization described here is not inconsistent with the function of Asp96 and Thr100 suggested from the comparison of the crystal structures of native and BMP ligated yeast ODCase (*19*). When ligand was bound, the polypeptide loop formed by residues 95−103 of the second subunit was repositioned to allow interactions among these residues, the ligand, and residues of its partner subunit that forms the active site. This movement enables contacts to be established with the 2′-OH of BMP and with the ϵ-amino group of the active site Lys93 in addition to placing the Asp96 γ-carboxylate in proximity to putative position of the carboxylate of OMP. These interactions, which are absent within individual subunits, could explain the obligatory relation between dimer formation and catalysis. Given the similarity in peptide fold observed for the mono functional ODCase proteins (19−21), the relationship between decarboxylation and ODCase domain dimerization described for the bifunction eukaryotic UMP synthase might also result from participation of residues from both ODCase domains in catalysis (*24*).

The addition of substrate to enzyme initially quenched the intrinsic protein fluorescence of E_2 yielding an enzyme−substrate complex designated E•S. After OMP was dearboxylated, the fluorescence of the enzyme returned to that of resting enzyme. The approach to the steady-state level of fluorescence quenching was a first-order process (Figure 3B). Thus, conversion of E to ES was a bimolecular process involving no intermediates formed after E•S with fluorescent properties significantly different from that of E•S. These observations suggested Scheme 3 appropriately described the kinetics of OMP decarboxylation by E_2 in which each subunit of E_2 functions independently. From an analysis of the value of the pseudo first-order rate constant for the approach to the steady-state, the value of k_{-1} was 60 s^{-1}. From this value and k_{cat} (15 s^{-1}) the commitment to catalysis (k_{cat}/k_{-1}) was estimated to be 0.25. This relatively low commitment to catalysis agreed with the observation of essentially a full ^{13}C-isotope effect (*14*, *15*).

The finding that E•S formation was readily reversible suggested that the release of products had not occurred during the formation of the complex with reduced fluorescence designated as E•S. This was confirmed by two observations. First, an enzyme equivalent of UMP was not formed in a burst as the steady-state was reached. Second, changes in $[H^+]$ during the course of the reaction were consistent with CO_2 being released as ES returned to resting enzyme. The effect of carbonic anhydrase on the time-course of $[H^+]$ changes indicated that CO_2 was released from the enzyme and not bicarbonate (Figure 6, panels A and B). The reaction catalyzed by E_2 is given by eq 11.

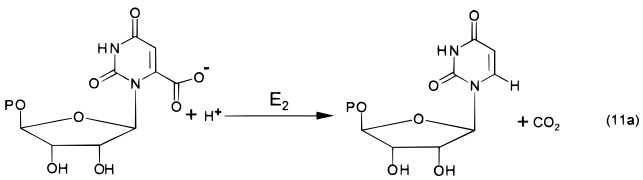

$$CO_2 + H_2O \longrightarrow H_2CO_3 \quad (11b)$$

$$H_2CO_3 \longrightarrow HCO_3^- + H^+ \quad (11c)$$

Because the hydration of CO_2 is slow in the absence of carbonic anhydrase (*27*), a proton was initially taken up from solvent during the decarboxylation of OMP by E_2 (eq 11a). Proton uptake was correlated with conversion of E•S to resting enzyme. The recovery of the proton consumed in the formation of UMP (eq 11a) occurred slowly as CO_2 was hydrated to H_2CO_3, which ionized rapidly to bicarbonate (pK = 3.8) as described by eqs 11b and 11c. Because most of the proton uptake did not occur in a burst prior to the conversion of E•S to resting enzyme, the substrate was not preferentially binding to a protonated form of the enzyme that was minor species at pH 7.2. When carbonic anhydrase was included in the single turnover experiment, proton uptake was nearly abrogated. This result suggested that CO_2 was released during the conversion of E•S to resting enzyme such that CO_2, following its hydration and ionization, compensated for the uptake of a proton observed during the decarboxylation reaction. However, the proton changes were not completely eliminated by carbonic anhydrase implying that a small fraction of the proton changes resulted from OMP sequestering a proton on the enzyme during the binding step. Nonetheless, CO_2 formation, proton uptake from solvent, and UMP formation occurred during the conversion of E•S to resting enzyme. Consequently, the enzymatic species (E•S) with reduced fluorescence represents the enzyme−substrate complex prior to the occurrence of chemistry at the C-6 position of the pyrimidine ring.

The pH dependence of k_{cat}/K_m gives information about the pK values on free enzyme and free substrate that are critical for binding (*28*). In the case of ODCase and OMP, the pK values determined were 6.1 and 7.7, which were similar to those values reported previously (*14*). Because of the difference in catalytic activity between the monomeric and dimeric form of the enzyme, the observed pK values in the pH rate profile could be the result of pH-dependent shifts in the monomer−dimer equilibrium of the enzyme. We considered this to be unlikely for the following reason. In the pH rate profile studies, the enzymatic reactions were initiated by dilution of enzyme equilibrated in 0.1 M NaCl and 0.5 mM MOPS at pH 7.2 into the buffer of interest. Thus, the enzyme was initially presented as a dimer to the substrate at the pH of interest. If the enzyme were dissociating into the monomer during the reaction, a time-dependent decrease in catalytic activity should have been observed. Because the time courses for product formation were linear over the first several seconds of the reaction at all pH values investigated, we have concluded that dissociation of dimeric enzyme to inactive monomeric enzyme was not the source of the observed pH dependencies.

From a comparison of substrate analogues with p*K* values differing from those of OMP, it was concluded that a negatively charged pyrimidine ring had a favorable interaction with the enzyme at low pH and an unfavorable interaction at high pH. This conclusion was based on the observation that a residue with a p*K* value of 8 was important for binding of substrate or substrate analogues to the enzyme whenever the p*K* of the pyrimidinyl moiety was less than 7.7−8. If the p*K* of the pyrimidinyl moiety was greater than 8 as was the case of $NH_2C(S)$UMP (pK = 8.7), the p*K* in the pH rate profile was shifted to a higher value. On the basis of X-ray structural data and mutagenesis (*6*, *9*), the ϵ-amino group of Lys-93 is an obvious candidate responsible for this p*K* in the pH rate profile data. The p*K* of this lysyl group, however, would have to be perturbed significantly from that of free lysine, possibly through its proximity to Asp-91 and Asp-96 in the active site (*19*). The lower p*K* (6.1 and 5.8) in the pH rate profile for OMP (pK = 6.1) and 6-$NH_2C(S)$UMP (pK = 5.8) was probably the p*K* of the phosphoryl group of the ligand (p*K* 6.2). For the yeast enzyme, the crystal structure shows that the phosphoryl group forms hydrogen bonds with the guanidinium group of Arg-235, the hydroxyl of Tyr-217, and the peptide amide of Gly-234 (*19*). These interactions are consistent with the phosphoryl dianion being the kinetically important species for ligand binding to enzyme (*19*). However, this p*K* can be overshadowed by ionization on the pyrimidinyl or purinyl ring. With 6-azaUMP, which has a p*K* value for ionization of the pyrimidinyl ring of 6.8, the value of the acid p*K* of the pH rate curve was shifted to 6.6. Similarly, the apparent p*K* value in the acid limb of the pH rate curve was shifted to 5.3 with 8-AzaXMP, which has a p*K* value for ionization of the purinyl ring of 4.5. If the value of the acid p*K* describing the pH rate profile were only the result of phosphoryl group ionization, then its value should have equaled that of the phosphoryl group [the p*K* values of the phosphoryl group of OMP, R-5-P, and UMP were 6.3 (Table 1)]. The observation that the value varied with varying purinyl analogues suggested that it was a complex function of ionizations of the purinyl ring and the phosphoryl group.

The bimolecular rate constant for association of E_2 with OMP or with substrate analogues approached the diffusion-controlled limit. It was surprising that 6-AzaUMP, which was sterically expected to be a good substrate analogue, had a value for k_1 (112 μM^{-1} s^{-1}) that was very similar to that (130 μM^{-1} s^{-1}) for the much bulkier analogue 8-AzaXMP. Bulky purine nucleotides such as AllopurinolMP had been reported earlier to be effective inhibitors of ODCase decarboxylase (*29*). These results were consistent with the openness or solvent accessibility of the active site seen in the crystal structure of unligated yeast enzyme (*19*). The K_d value of substrate analogue was more dependent on the value of the dissociation rate constant than the value of the association rate constant (Table 1). Values for the dissociation rate constants for the five substrate analogues tested, varied 3 orders of magnitude, whereas the values for the association rate constants varied over only 1 order of magnitude. Thus, the relative stability of the E−ligand complex was determined largely by the value of the dissociation rate constant, which in turn was determined by attractive forces between the ligand and enzyme. The value of the dissociation rate constant of E•UMP was not determined directly. However, it could be calculated from the value of the K_i (450 μM) and an estimated value for the association rate constant that was a median value of the association rate constants for the inhibitors of Table 1 ($\sim$50 μM^{-1} s^{-1}). From these values, the dissociation rate constant of E•UMP was $\sim$20 000 s^{-1}, which was 300-fold greater than the value for E•OMP and over 5×10^6-fold greater that the value for E•6-$NH_2C(S)$-UMP (Table 1). These results suggested than strongly attractive forces between enzyme and the substrate were dissipated during the decarboxylation of OMP. Furthermore, the kinetic data presented herein were consistent with the formation of E•S that subsequently reverted to resting enzyme with concerted proton uptake, UMP formation, and CO_2 release occurring with reversal of the fluorescence change observed during the formation of E•S. Thus, dimeric ODCase must direct the potential forces associated with formation of E•S into decarboxylation of the OMP in a functionally single-stepped process.

ACKNOWLEDGMENT

We thank B. Miller for informative discussions during the course of this work and T. Kalman for the gift of the 6-$NH_2C(S)$UMP used in these studies. We also thank M. Moyer for performing the quantitative amino acid analysis on the enzyme.

REFERENCES

1. Lieberman, I., Kornberg, A., and Simms, E. S. (1955) *J. Biol. Chem. 215*, 403−415.
2. Radzicka, A., and Wolfenden, R. (1995) *Science 267*, 90−93.
3. Miller, B. G., Smiley, J. A., Short, S. A., and Wolfenden, R. *J. Biol. Chem.* (1999) *274*, 23841−23843.
4. Cui, W., DeWitt, J. G., Miller, S. M., and Wu, W. (1999) *Biochem. Biophys. Res. Commun. 259*, 133−135.
5. Umezu, K., Amaya, T., Yoshimoto, A., and Tomita, K. (1971) *J. Biochem. 70*, 249−262.
6. Smiley, J. A., and Jones, M. E. (1992) *Biochemistry 31*, 12162−12168.
7. Miller, B. G., Traut, T. W., Wolfenden, R. (1999) *Bioorg. Chem. 26*, 283−288.
8. Smiley, J. A., and Saleh, L. (1999) *Bioorg. Chem. 27*, 297−306.
9. Bell, J., and Jones, M. E. (1991) *J. Biol. Chem. 266*, 12662−12667.
10. Beak, P., and Segal, B. (1976) *J. Am. Chem. Soc. 98*, 3601−3606.
11. Lee, J. K., and Houk, K. N. (1997) *Science 276*, 942−945.
12. Silverman, R. B., and Groziak, M. P. (1982) *J. Am. Chem. Soc. 104*, 6434−6439.
13. Acheson, S. A., Bell, J. B., Jones, M. E., and Wolfenden, R. (1990) *Biochemistry 29*, 3198−3202.
14. Smiley, J. A., Paneth, P., O'Leary, M. H., Bell, J. B., and Jones, M. E. (1991) *Biochemistry 30*, 6216−6223.
15. Ehrlich, J. I., Hwang, C.-C., Cook, P. F., and Blanchard, J. S. (1999) *J. Am. Chem. Soc. 121*, 6966−6967.
16. Levine, H. L., Brody, R. S., and Westheimer, F. H. (1980) *Biochemistry 19*, 4993−4999.
17. Shostak, K., and Jones, M. E. (1992) *Biochemistry 31*, 12155−12161.
18. Yablonski, M. J., Pasek, D. A., Han, B.-D., Jones, M. E., and Traut, T. W. (1996) *J. Biol. Chem. 271*, 10704−10708.
19. Miller, B. G., Hassell, A. M., Wolfenden, R., Milburn, M. V., and Short, S. A. (2000) *Proc. Nat. Acad. Sci. U.S.A. 97*, 2011−2016.
20. Appleby, T. C., Kinsland, C., Begley, T. P., and Ealick, S. E. (2000) *Proc. Nat. Acad. Sci U.S.A. 97*, 2005−2010.

21. Wu, N., Mo, Y., Gao, J., and Pai, E. F. (2000) *Proc. Nat. Acad. Sci. U.S.A. 97*, 2017−2022.
22. Feng, W. Y., Austin, T. J., Chew, F., Gronert, S., and Wu, W. (2000) *Biochemistry 39*, 1778−1783.
23. Gittelman, M. S., Matthews, C. R. (1990) *Biochemistry 29*, 7011−7020.
24. Segal, I. H. (1975) *Enzyme Kinetic*s, p 73, John Wiley & Sons Inc., New York.
25. Cody, V., and Kalman, T. I. (1985) *Nucleosides Nucleotides 4*, 587−594.
26. Traut, T. W., and Payne, R. C. (1980) *Biochemistry 19*, 6068−6074.
27. Jonsson, B. H., Steiner, H., Lindskog, S. (1976) *FEBS Lett. 64*, 310−314.
28. Segal, I. H. (1975) *Enzyme Kinetics*, pp 884−941, John Wiley & Sons Inc., New York.
29. Fyfe, J. A., Miller, R. L., and Krenitsky, T. A. (1973) *J. Biol. Chem. 248*, 3801−3809.

BI001199V